ELSEVIER

Thermochimica Acta 303 (1997) 197–202

thermochimica acta

DTA investigation of the retrogression and re-ageing in some AlZnMgCu alloys

Andrzej Gazda*, Małgorzata Warmuzek, Wojciech Wierzchowski

Foundry Research Institute, 30-418 Kracow, 73 Zakopianska, Poland

Received 25 February 1997; received in revised form 13 June 1997; accepted 7 July 1997

Abstract

High strength AlZnMgCu alloys of greater magnesium content than usually in 7000 series were examined. An analysis of multi-stage heat treatments involving retrogression and re-ageing (RRA) was performed. The phase transformations proceeding during subsequent steps of that complex heat treatment were studied using differential thermal analysis (DTA) and electrical resistance measurements. Based on the behaviour of dissolution processes of particles strengthening the solid solution, the optimum parameters of RRA were determined and good mechanical properties were achieved. The measurements of electrical resistance at ambient temperature enabled establishing optimum conditions of retrogression (temperature and time), affecting the mechanical properties and specific electrical resistivity, which are considered to be a good measure of the alloy's susceptibility to stress corrosion cracking. © 1997 Elsevier Science B.V.

Keywords: Ageing; Aluminium alloys; DTA; Retrogression

1. Introduction

The high strength AlZnMgCu alloys, based on the ternary AlZnMg system, applied in the airplane and machine industry (7000 series), are produced in cast and wrought states alike.

Many efforts were made to explain the influence of chemical composition and thermal treatment on the microstructure, determining the mechanical properties of AlZnMgCu alloys [1–5].

Alloys solidifying under real conditions, when the solubility of constituents depends on temperature, are characterized by a non-equilibrium phase constitution and by the structural as well as chemical heterogeneity of solid solution. The heat treatment applied to aluminium alloys of the 7000 series, for strengthening the matrix by means of precipitation from the supersaturated solid solution (SSS), is composed of two main, consecutive stages:

- homogenization, affecting the morphology and phase composition of constituents of the alloy;
- supersaturation and ageing, affecting the state of the solid solution.

In the ternary AlCuMg system, the decomposition of the supersaturated solid solution depends on the ratio of Cu/Mg [6,7] and if Cu/Mg < 1, it proceeds as follows: SSS $\rightarrow$ GPB $\rightarrow$ S″ (intermediate phase) $\rightarrow$ S′ (semicoherent phase) $\rightarrow$ S (stable Al_2CuMg phase); where GPB are cylindrical GP zones containing Cu and Mg atoms. If Cu/Mg ≈ 0.4, then the dominant

*Corresponding author. Fax: 0048 012 66 54 78; e-mail: agazda@iod.krakow.pl

PII S0040-6031(97)00254-2

phase is T (Al_6CuMg_4). If Cu/Mg > 1, then GPB and GPI (AlCu) zones co-exist, or only one kind of Mg-rich GP zones with their composition depending on the Cu/Mg ratio appears. In particular, if the ratio Cu/Mg > 8, then phase Θ (Al_2Cu) prevails.

In the ternary system AlZnMg, several paths of decomposition of the supersaturated solid solution are considered [8,9]:

1. nucleation and growth of GP zones

$$\text{SSS} \rightarrow \text{GP zones} \rightarrow \eta'(\text{intermediate phase}) \rightarrow \eta(\text{stable } MgZn_2)$$

2. nucleation on defects and grain boundaries

$$\text{SSS} \rightarrow T\,(\text{stable at high ageing temperature})(Al,Zn)_{49}Mg_{32}) \rightarrow \eta$$

3. nucleation on vacancy rich clusters (VRC)

$$\text{SSS} \rightarrow \text{"nuclei"} \begin{matrix} \rightarrow T \\ \rightarrow \eta' \rightarrow \eta \end{matrix}$$

Addition of copper facilitates and accelerates nucleation of GP zones and η' phase, without changing the decomposition sequence of the solid solution.

It is known that, invented by B. Cina [10], multistage heat treatments, involving retrogression and re-ageing, allow to dissolve unstable precipitates and modify (coarsen) the η precipitates in the grain boundaries changing their shape, size and electrochemical properties. It leads to the improvement of some properties of the alloy (i.e. susceptibility to the stress corrosion cracking), while retaining its high strength [11]. RRA consists of several steps as follows:

- solution of heat treatment and quenching,
- ageing to peak hardness (standard T6 heat treatment),
- retrogression, i.e. holding the alloy for a short time at a temperature above the ageing temperature,
- re-ageing at the T6 ageing temperature.

The results of this modification, i.e. a change in the structure of grain boundary precipitates, can exert an influence on several, structure-sensible, thermophysical properties. Electrical conductivity – expressed in % IACS as an alloy conductivity ratio to the 'international annealed copper standard' – is accepted to provide an indication for the alloy's susceptibility to stress corrosion cracking.

The aim of this paper is to follow the precipitation processes during retrogression and re-ageing by means of differential thermal analysis. Calorimetric identification of the precipitates and description of the decomposition sequence of the supersaturated solid solution in Al-based alloys are well established experimentally, especially with the aid of differential scanning calorimetry (DSC) studies [12–16], but lack of comprehensive calorimetric studies of the heat treatment problems in AlZnMgCu alloys should be noticed.

In an earlier work [16], the authors were concerned with the metallographic investigation of primary structures in the as-cast state in some AlZnMgCu alloys, analysed the process of homogenization and established the precipitation sequence of the non-equilibrium structural components in the liquidus–solidus temperature range. It has been a good starting point to establish the parameters (temperature and time) of the homogenization heat treatment.

2. Materials and experimental procedure

Chemical composition of the examined alloys is given in Table 1. From the castings made by squeeze-casting technology the specimens for the electrical resistivity and DTA measurements, microscopic investigations and static tensile tests were cut out and prepared.

Based on the preliminary DTA studies and the authors' previous work [16], the following conditions of a T6 heat treatment were chosen:

- homogenization: 450°C/5 h,
- supersaturation: 470°C/1 h → water quenching,
- ageing: 120°C/24 h.

Table 1
Chemical composition of examined alloys (Al-balance)

Alloy	Mg in wt%	Zn in wt%	Cu in wt%
A	1.25	6.10	2.36
B	2.13	6.00	2.35
C	3.63	6.10	2.33

After this initial heat treatment, the material was subjected to the retrogression process. Two series of experiments were made according to the scheme:

- retrogression $R(1)$: $T_r = 180°C$, time of retrogression $t_r = 5, 10, 15, 20, 30, 40, 60, 70$ min and re-ageing according to T6 temper,
- retrogression $R(2)$: $T_r = 200°C$, time of retrogression $t_r = 2, 5, 7, 10, 15, 20, 30, 40, 50$ min and re-ageing according to T6 temper.

For the examined Alloys A, B and C, after each stage of the heat treatment described by the temperature and time of retrogression, the measurements of electric resistivity and DTA were made.

An analysis of the specific electrical resistivity ρ at ambient temperature (25°C) was performed on cylindrical specimens Φ 3.5 × 50 mm, using a precise RFT Thomson resistance bridge.

Thermal analysis was performed in a Linseis L75 DTA apparatus in combination with a Linseis Data Acquisition System L8500, at a heating rate of 5 K/min. DTA measurements were carried out in pure argon, using alumina crucibles, on specimens of Φ 3.5 × 8 mm and with aluminium samples as a reference. The DTA calibration was performed by measuring the heat of melting of pure elements (In, Sn) using the same working conditions; the base line was determined by performing measurements on two Al-samples.

3. Electrical resistivity measurements

Figs. 1–3 present the specific electrical resistivity vs. time of retrogression for Alloy A, Alloy B and Alloy C, respectively. The error of each experimental point does not exceed 1%. For the examined Alloys A, B and C specific electrical resistivity at ambient temperature increases with magnesium content in the alloy. In general, specific electrical resistivity decreases (conductivity rises) with time of retrogression; characteristic resistivity maximum due to partial dissolution of unstable precipitates was recorded only for Alloy B retrogressed at 200°C (Fig. 2(b)).

4. DTA measurements

Figs. 4–6 show DTA runs for Alloys A, B and C after supersaturation (quenched) and after ageing (T6). The analysis of DTA curves after the consecutive steps of heat treatment: homogenization and supersaturation, ageing, retrogression and re-ageing yields the following qualitative remarks.

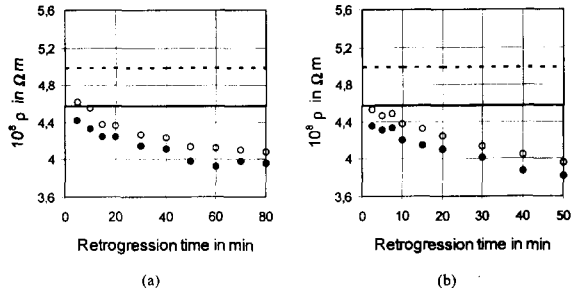

Fig. 1. Specific electrical resistivity of Alloy A vs. retrogression time after quenching (dotted line), ageing (solid line), retrogression (blank circles) and re-ageing (black circles); (a) retrogression $R(1)$ at 180°C, (b) retrogression $R(2)$ at 200°C.

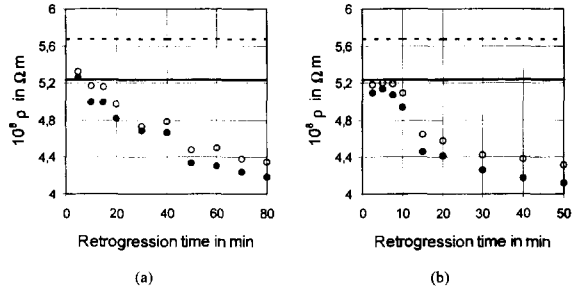

Fig. 2. Specific electrical resistivity of Alloy B vs. retrogression time after quenching (dotted line), ageing (solid line), retrogression (blank circles) and re-ageing (black circles); (a) retrogression $R(1)$ at 180°C, (b) retrogression $R(2)$ at 200°C.

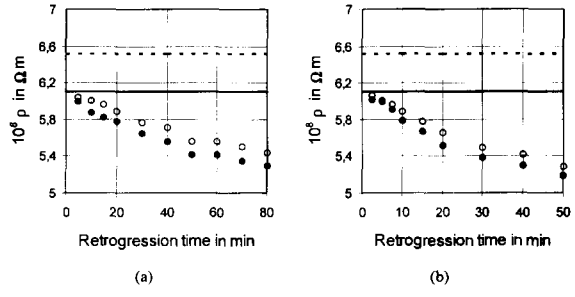

Fig. 3. Specific electrical resistivity of Alloy C vs. retrogression time after quenching (dotted line), ageing (solid line), retrogression (blank circles) and re-ageing (black circles); (a) retrogression $R(1)$ at 180°C, (b) retrogression $R(2)$ at 200°C.

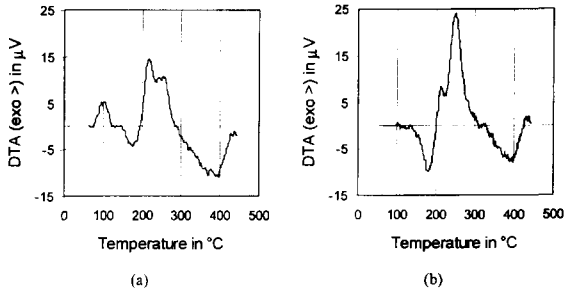

Fig. 4. Thermoanalytical curve of Alloy A after (a) quenching (b) ageing.

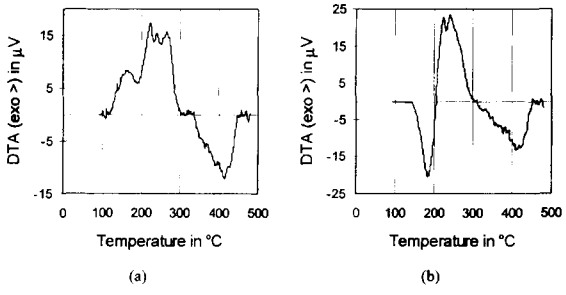

Fig. 5. Thermoanalytical curve of Alloy B after (a) quenching (b) ageing.

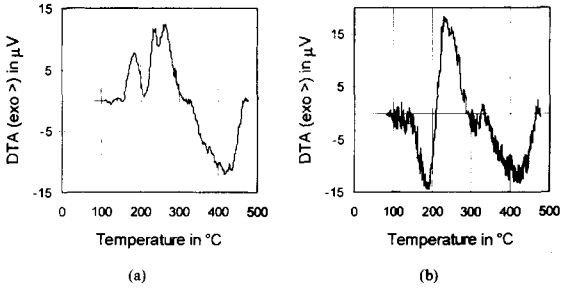

Fig. 6. Thermoanalytical curve of Alloy C after (a) quenching (b) ageing.

4.1. Supersaturated (quenched) alloy

Based on previous DSC and transmission electron microscopy (TEM) investigations [12–15] and peaks' maxima temperature evaluation, exothermic peaks (Figs. 4(a)–6(a)), with maximum below 200°C are connected with formation of GP zones and metastable phase η'. The next, higher temperature thermal effects (200–300°C) of more complex shapes are a superposition of exothermic effects of precipitation of stable phase η and endothermic ones of dissolution of phase η'. The formation of the metastable phase η' either on vacancy rich clusters (VRC) or via growth of GP zones, results in a double dissolution peak of that phase. The broad, endothermic peaks present dissolution of stable phase η.

4.2. Alloy aged at 120°C for 24 h

In this case there is a fine precipitate structure connected with strengthening the alloy's matrix with GP zones and η'. The DTA runs (Fig. 4(b)–6(b)) are different from those of supersaturated specimens. There are no precipitation peaks of coherent and semicoherent phases, but the endothermic dissolution effects of these phases (maximum at ca. 180°C) are very distinct, being a very good measure of the quantity of coherent and semicoherent precipitates resulting in the precipitation hardening of the alloy. Exothermic effects (precipitation of η phase) are slightly disturbed by dissolution of η'.

4.3. Alloy retrogressed at 180°C and 200°C

Thermoanalytical curves are similar to those obtained for condition T6, but have some very interesting features. As an example, Alloy B is taken into consideration. The maxima of metastable phase dissolution peaks are moved to higher temperatures (180°C → 210°C) with increasing time of retrogression (Figs. 7 and 8), due to coarsening of precipitates.

For longer times of retrogression small exothermic effects can be observed (Fig. 7(b)), mainly in specimens after $R(2)$ retrogression (Fig. 8(b)). They are

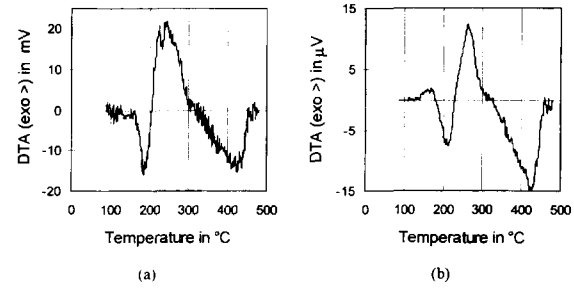

Fig. 7. Thermoanalytical curve of Alloy B after retrogression at 180°C; (a) 5 min (b) 80 min.

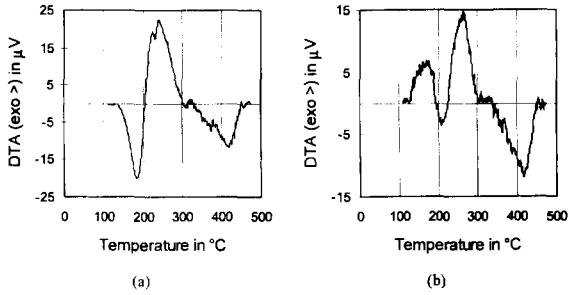

Fig. 8. Thermoanalytical curve of Alloy B after retrogression at 200°C; (a) 2 min (b) 30 min.

Table 2
Mechanical properties of examined alloys after different versions of the heat treatment

Alloy	Description of heat treatment	Ultimate tensile strength in MPa	Elongation in %
A	ageing 120°C/24 h	469	9.9
	R(1)RA, t_r = 20 min	499	11.0
	R(2)RA, t_r = 10 min	472	5.8
B	ageing 120°C/24 h	504	4.9
	R(1)RA, t_r = 20 min	527	6.0
	R(2)RA, t_r = 10 min	530	5.5

caused by the progressive dissolution of GP zones and η'-phase during retrogression and subsequent precipitation of metastable η' during the DTA measurement.

4.4. *Retrogressed and re-aged alloy*

The thermoanalytical curves show a similarity to those recorded for retrogressed alloys as the shift of maximum of dissolution peaks is also observed, and differ from those achieved for retrogressed alloy as the low-temperature exothermic effects are not observed.

5. Mechanical properties

The results of the present work were applied to test the influence of the RRA heat treatment parameters on some mechanical properties of the examined Alloys A and B. Finally, static tensile testing of the material after established RRA heat treatment was carried out at ambient temperature. The results of the measurements are summarized in Table 2.

6. Discussion

The temperature shift of the dissolution peaks of matrix strengthening phases and a decrease of specific electrical resistivity with time of retrogression prove the partial dissolution of the unstable precipitates in the matrix and the coarsening of precipitates during retrogression.

The decrease of the specific resistivity with time of retrogression indicates a reduction of susceptibility to stress corrosion cracking. The lower, accepted limit 36% IACS corresponds to a specific electrical resistivity $\rho = 4.8 \times 10^{-8}$ Ωm. The condition of minimum electrical conductivity (maximum resistivity) is always fulfilled for Alloy A, satisfied for Alloy B (depending on time of retrogression) but never occurs for Alloy C. The specific electrical resistivity measurements show that, from the point of view of reduction of susceptibility to stress corrosion cracking by means of the RRA process, it is only reasonable in Alloys A and B to look for an optimum in mechanical properties.

The endothermic thermal dissolution effects of precipitates causing the strengthening of the alloy were chosen to characterize the alloys' decomposition status after ageing, retrogression and re-ageing. The values of the enthalpy change have been measured with an uncertainty of 6%. Fig. 9(a and b) demonstrate the dependence of the heat of dissolution of GP zones and η' on the time of retrogression for Alloy A, retrogressed at 180°C and 200°C, respectively.

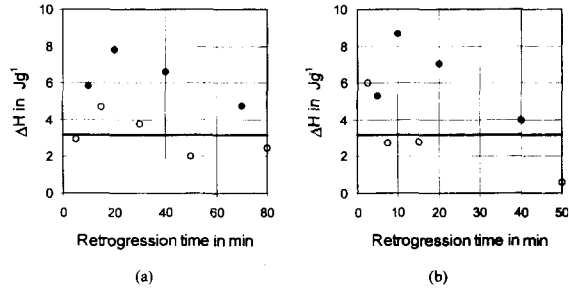

Fig. 9. Heat of dissolution of dispersive in Alloy A vs. retrogression time after ageing (solid line), retrogression (blank circles) and re-ageing (black circles); (a) retrogression R(1) at 180°C. (b) retrogression R(2) at 200°C.

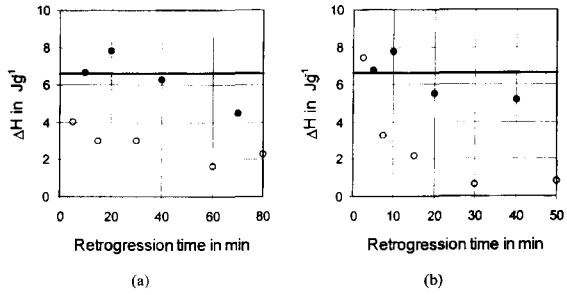

Fig. 10. Heat of dissolution of dispersive precipitates in Alloy B vs. retrogression time after ageing (solid line), retrogression (blank circles) and re-ageing (black circles); (a) retrogression $R(1)$ at 180°C, (b) retrogression $R(2)$ at 200°C.

Fig. 10(a and b) show the same relationships for Alloy B. These relationships are found to be similar to those obtained for the hardness after RRA in a 7150 Al alloy [11].

A distinct maximum for $t_r = 20$ min ($T_r = 180$°C) and $t_r = 10$ min ($T_r = 200$°C) can be found for Alloy A and Alloy B.

For the samples submitted to re-ageing, the appearance of a maximum in the relationship – dissolution heat of matrix strengthening phases vs. time of retrogression – indicates that there exists a maximum quantity of matrix strengthening phases for definite T_r and t_r. At these points the condition of maximum specific electrical resistivity ensuring a sufficient resistance to stress corrosion cracking is also fulfilled.

The low temperature exothermic DTA effects observed after retrogression are caused by precipitation of η' during non-isothermal ageing in the DTA apparatus. They indicate that in spite of the partial dissolution (reversion) of the metastable precipitates during retrogression, the remaining act as nucleation sites for the η' particles. That phenomenon, not recorded for small enthalpy changes after short times of retrogression, should also proceed for shorter times of retrogression. It is quite evident that the same process of precipitation occurs during the last step of the heat treatment (re-ageing).

It affects re-precipitation of the matrix strengthening phase during re-ageing and results in a significant modification of the alloy microstructure as compared with the state after one-step ageing.

The mechanical properties obtained for Alloys A and B (retrogressed at a 'maximum of dissolution heat') are better (with the exception of Alloy A at point 200°C, 10 min) than those obtained after standard T6 temper. It proves that structure and distribution of the precipitates are more favourable from the point of view of the precipitation strengthening.

7. Conclusions

The multi-stage heat treatment characterized by retrogression and re-ageing allows the status of strengthening and grain boundary precipitates to be modified on a larger scale than by standard T6 temper. The coarsening of grain boundary precipitates achieved during retrogression step can be balanced with re-precipitation of the matrix strengthening phase during re-ageing.

Based on the results of the work for Alloys A and B, it is possible to choose the parameters of RRA heat treatment in a way to obtain the minimum conductivity (maximum resistivity) indicating admissible susceptibility to stress corrosion cracking and better mechanical properties, than in the case of T6 condition.

References

[1] T. Staley, Metall. Trans., 5 (1974) 929.
[2] C.Q. Chen, Strength of Metals and Alloys, 1 (1986) 459.
[3] S.R. Arumalla, Strength of Metals and Alloys, 1 (1986) 453.
[4] P. Archambault, Strength of Metals and Alloys, 1 (1986) 447.
[5] Li Qingchum, Strength of Metals and Alloys, 2 (1986) 1651.
[6] M. Silcock, J. Inst. Metals, 89 (1960/61) 203.
[7] V. Ratchev, Scripta Met., 30 (1994) 599.
[8] J.D. Embury, R.B. Nicholson, Acta Met., 13 (1965) 403.
[9] N. Ryum, Z. Metallk., 66 (1975) 338.
[10] B. Cina, U.S. Patent No. 3, 856, 584, Dec 24, 1974.
[11] M.B. Hall, J.W. Martin, Z. Metallk., 85 (1994) 134.
[12] J.K. Ardell, J.K. Park, Mat. Sci. Eng. A, 114 (1989) 197.
[13] C. Garcia-Cordovilla, Mater. Sci. Eng., A132 (1991) 135.
[14] S. Nebitt, D. Hamana, G. Cizeron, Acta Metall. Mater., 43 (1995) 3583.
[15] W. Lacom, Thermochim. Acta, 271 (1996) 93.
[16] M. Warmuzek, A. Gazda and W. Wierzchowski, 11th Congress on Mat. Test. Balatonszeplak, 1994, Conf. Proc., Vol. IV, p. 1325.